

# Lymphotoxin Pathway and Aire Influences on Thymic Medullary Epithelial Cells Are Unconnected<sup>1</sup>

Emily S. Venanzi, Daniel H. D. Gray, Christophe Benoist, and Diane Mathis<sup>2</sup>

The lymphotoxin pathway is critical for the development and maintenance of peripheral lymphoid organs. Mice with deficiencies in members of this pathway lack lymph nodes and Peyer's patches and have abnormal spleen architecture. These animals also develop autoantibodies to and lymphocytic infiltrates of multiple organs, provoking speculation that the lymphotoxin pathway may play a role in central tolerance induction. Indeed, a series of reports has claimed that lymphotoxin signals control the expression of Aire, a transcriptional regulator that is expressed in medullary epithelial cells of the thymus, mediates ectopic transcription of genes encoding a variety of peripheral tissue Ags, and promotes clonal deletion of self-reactive thymocytes. However, one report argued that lymphotoxin signals regulate the composition and organization of the thymus, particularly of the medullary epithelial compartment. Herein, we resolve this controversy in favor of the latter view. The expression and function of Aire were unaffected in medullary epithelial cells of mice lacking either lymphotoxin  $\beta$  receptor or the lymphotoxin  $\alpha$ -chain, and there was minimal overlap between the sets of genes controlled by Aire and lymphotoxin. Instead, both knockout lines showed abnormal medullary epithelial cell organization, and the line lacking the  $\beta$  receptor had significantly fewer medullary epithelial cells. In short, the lymphotoxin pathway drives the developmental rather than selectional properties of thymic stromal cells. *The Journal of Immunology*, 2007, 179: 5693–5700.

Lymphotoxin (LT)<sup>3</sup>  $\beta$  receptor, a TNFR superfamily member, is a key mediator of the genesis and maintenance of peripheral lymphoid tissues (1). It binds to the trimeric ligands LT $\alpha$ 1 $\beta$ 2 and LIGHT and signals through TNFR-associated factors, intracellular zinc RING finger signal transducers upstream of the NF- $\kappa$ B family of transcription factors (2). Within the NF- $\kappa$ B family, the p50/RelA and p52/RelB arms are activated by LT $\beta$ R (3), leading to the expression of many genes that regulate inflammation and lymphoid organ development and organization.

Mice deficient for the ligands and receptors of the LT pathway revealed the importance of these factors for the peripheral lymphoid system. LT $\alpha$  (4), LT $\beta$  (5), and LT $\beta$ R (6) single knockouts (KOs) all lack Peyer's patches and most lymph nodes and have disorganized spleens. They also develop lymphocytic infiltrates of (6, 7), and produce autoantibodies against (8, 9), peripheral tissues, although the cause of this phenomenon remains unknown.

Less is known about the role of the LT pathway in the thymus. Mice deficient in factors downstream of LT $\beta$ R, including NF- $\kappa$ B-inducing kinase and RelB, exhibit a disrupted thymic architecture (10–12). These results, coupled with the observation that the LT pathway is crucial for normal peripheral lymphoid organ development, suggested that this pathway might also be important in the development and organization of the thymus. In addition, the tissue infiltrates and autoantibodies in LT-deficient mice have provoked speculation that the pathway may be involved in central tolerance induction. Thymocytes express the ligands LT $\alpha$ 1 $\beta$ 2 (13) and LIGHT (14), while LT $\beta$ R is displayed by medullary epithelial cells (MECs) (15). MECs are thymic stromal cells that also express a wide array of peripheral tissue Ags (PTAs) (16), many of whose RNA transcripts are controlled by the transcriptional regulator Aire (17). Aire-deficient mice also develop lymphocytic infiltrates and autoantibodies (17, 18), exhibiting a phenotype somewhat similar to that of the LT KOs. This observation led to the suggestion that the LT and Aire influences may be somehow connected.

Two groups have examined the role of the LT pathway in the composition/structure of the thymic epithelium, Aire expression, and PTA gene transcription and came to conflicting conclusions. Boehm et al. (8) concluded that LT $\beta$ R signals are required for proper MEC differentiation and organization, while the second group, led by Fu (9, 19, 20), contended that signals through LT $\beta$ R regulate *aire* and PTA gene transcription and not thymus epithelium composition/structure. The latter view seems to have gained widespread acceptance (21–28). In this study, we directly addressed these conflicting conclusions and further examined the role of the LT pathway in the thymus and its relationship to *aire* and PTA gene transcription, using a combination of histologic, flow cytometric, and gene expression-profiling approaches.

## Materials and Methods

### Mice

Aire-deficient mice were derived and genotyped as previously described (17) and backcrossed to the B6 strain for at least nine generations before intercrossing. LT $\alpha$ -deficient mice (7) on the B6 background were obtained

Department of Medicine, Section on Immunology and Immunogenetics, Joslin Diabetes Center, Brigham and Women's Hospital; Harvard Medical School, Boston, MA 02215

Received for publication May 14, 2007. Accepted for publication September 5, 2007.

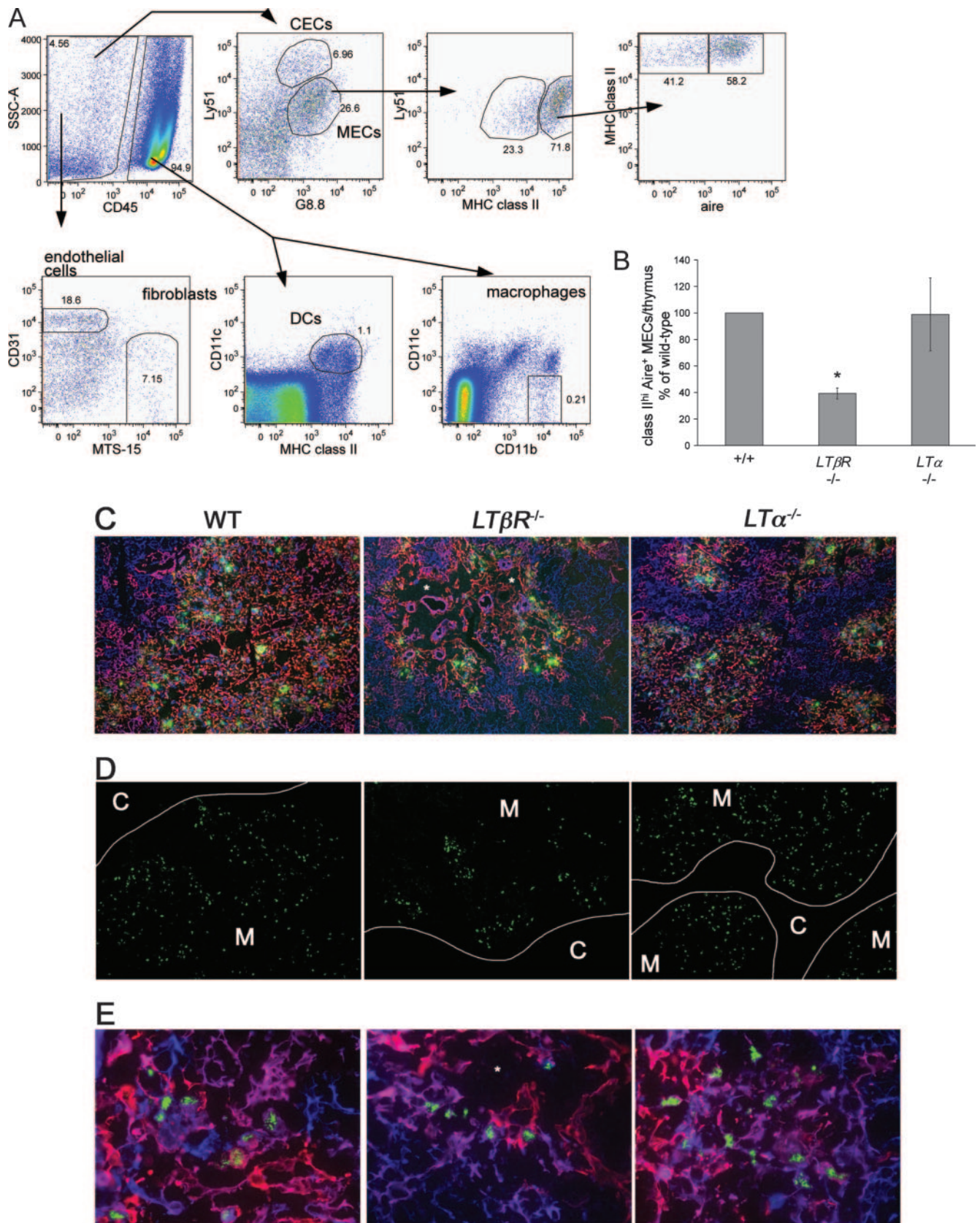
The costs of publication of this article were defrayed in part by the payment of page charges. This article must therefore be hereby marked *advertisement* in accordance with 18 U.S.C. Section 1734 solely to indicate this fact.

<sup>1</sup> This work was supported by National Institutes of Health Grant RO1 DK60027 and Young Chair funds (to D.M. and C.B.) and by Joslin's National Institutes of Diabetes and Digestive and Kidney Diseases-funded Diabetes and Endocrinology Research Center core facilities. E.S.V. received support from National Institutes of Health Training Grant T32 DK07260 and D.H.D.G. received support from an Australian National Health and Medical Research Council C. J. Martin Overseas Biomedical Fellowship.

<sup>2</sup> Address correspondence and reprint requests to Dr. Christophe Benoist and Dr. Diane Mathis, Section on Immunology and Immunogenetics, Joslin Diabetes Center, One Joslin Place, Boston, MA 02215. E-mail address: ebdm@joslin.harvard.edu

<sup>3</sup> Abbreviations used in this paper: LT, lymphotoxin; KO, knockout; PTA, peripheral tissue Ag; MEC, medullary epithelial cell; WT, wild type; CEC, cortical epithelial cell; K, keratin; UEA-1, *Ulex europaeus* agglutinin 1; FC, fold change; CII, type II collagen; RIP, rat insulin promoter; MFI, mean fluorescence intensity; DC, dendritic cell.

Copyright © 2007 by The American Association of Immunologists, Inc. 0022-1767/07/\$2.00



from The Jackson Laboratory; *LTβR*-deficient mice on the B6 background were a gift from Dr. Y.-X. Fu (University of Chicago, Chicago, IL). For each KO line, heterozygotes were bred to each other and resulting KO and WT littermate control animals were used for the experiments in this study, unless otherwise noted. All experiments in this study were approved by the Harvard University Institutional Animal Care and Use Committee.

### Thymus digestion and MEC sorting

Thymic epithelial cells MEC prepared according to a previous study (29) for phenotypic analysis by flow cytometry. Thymi from individual mice were serially digested, and the resulting single-cell suspensions were counted and used for staining and analysis on an LSR II flow cytometer (BD Biosciences). Thymic epithelial cells for microarray analysis were prepared according to a previous report (17). Individual thymi from young adult (3- to 5-wk-old) animals were digested, separated by density gradient centrifugation, and the thymic epithelial cell-enriched fraction was harvested and stained for sorting. MECs were sorted on a MoFlo cell sorter (DakoCytomation) according to the phenotype  $CD45^{-}G8.8^{+}Ly51^{int}I-A^{b}Igh$ .

### Thymocyte analysis

Individual thymi were pushed through 40- $\mu$ m mesh, liberating thymocytes, which were then washed and stained for analysis on an LSR II flow cytometer.

### Abs and staining

All staining began with an incubation with the anti-FC $\gamma$ R Ab 2.4G2. For intracellular staining, fixation/permeabilization buffers from eBioscience were used per the manufacturer's instructions. Abs used for MEC isolation for microarray analysis were anti-CD45-allophycocyanin (clone 30-F11), anti-Ly51-PE (clone BP-1), anti-I-A<sup>b</sup>-FITC (clone AF6-120.1; all from BD Pharmingen), and anti-EpCam-biotin (clone G8.8a; Developmental Studies Hybridoma Bank, University of Iowa, Iowa City, IA). Also used was streptavidin-PE-Cy7 from BD Pharmingen. Additional Abs used for thymus cell subset analyses were anti-CD45-PerCP-Cy5.5 (clone 30-F11) and anti-CD11c-PE (clone HL3) from BD Pharmingen; anti-I-A/E-Pacific Blue (clone M5/114.15.2) from BioLegend; anti-EpCam-APC (clone G8.8a); anti-CD11b-FITC (clone M1/70) from eBioscience; anti-CD31-FITC (clone 390) and anti-rat IgG2c-PE and -FITC (clone 2C 8F1) from Southern Biotechnology Associates; MTS-15 (rat IgG2c supernatant); and anti-*Aire* (rat IgG2c clone 5H12; gift from Dr. H. Scott, Walter and Eliza Hall Institute, Melbourne). Additional Abs used for thymocyte analyses were anti-CD4-PE-Cy7 (clone RM4-5) and anti-CD8 $\alpha$ -allophycocyanin-Alexa750 (clone 5H10) from Caltag Laboratories; anti-V $\alpha$  2-FITC (clone B20.6) and anti-V $\beta$  5-PE (clone MR9.4) from BD Pharmingen; and anti-Foxp3-allophycocyanin (clone FJK-16S) from eBioscience. Additional Abs used for immunohistology were biotin-conjugated rat anti-mouse K8 (clone TROMA-1) from the Developmental Studies Hybridoma Bank; rabbit anti-mouse K5 from Covance Research Products; Cy3-conjugated donkey anti-rabbit IgG from Jackson ImmunoResearch Laboratories; and allophycocyanin-conjugated streptavidin from BD Pharmingen.

### Immunohistology

Air-dried cryosections of thymus (8  $\mu$ m) were stained with titrated concentrations of primary Abs for 30 min, then subjected to three 5-min washes in PBS. Secondary Abs were incubated for 30 min followed by further washes and mounting with coverslips in aqueous mounting medium (Biomedex). Images were acquired on an Axiovert 200M confocal microscope (Zeiss) using a xenon arc lamp in a Lambda DG-4 wavelength switcher (Sutter Instrument) and processed with Slidebook imaging software (Intelligent Imaging).

### RNA isolation

Total RNA was prepared from the sorted MECs using the TRIzol reagent (Invitrogen Life Technologies). The standard manufacturer's protocol for isolation of total RNA from cultured cells was followed. RNA was resus-

pended in sterile, RNase-free water. It was quantitated using the NanoDrop ND-1000 spectrophotometer (NanoDrop Technologies).

### RNA amplification and microarray hybridization

Total MEC RNA was amplified using a T7 polymerase-based method. First- and second-strand cDNA synthesis, *in vitro* transcription of complementary RNA, and a second round of first- and second-strand cDNA synthesis were performed using a MessageAmp aRNA Kit (Ambion) as directed. The resulting cDNA was used in a second round of *in vitro* transcription, performed using the BioArray High Yield RNA Transcript Labeling Kit (Enzo Diagnostics) as directed, incorporating biotinylated ribonucleotides into the aRNA. The labeled aRNA was purified using the RNeasy Mini Kit (Qiagen). A 5 $\times$  fragmentation buffer (200 mM Tris-acetate (pH 8.1), 500 mM KOAc, 150 mM MgOAc) was added to 15  $\mu$ g of the biotinylated aRNA, and this mixture was heated at 94°C for 35 min. Fragmented samples were then hybridized to Affymetrix Mouse Genome 430 2.0 chips. The arrays were hybridized for 16 h at 45°C with constant rotation at 60 rpm. Next, they were washed and conjugated with streptavidin-PE in the Fluidics Station 400 (Affymetrix). Finally, each chip's fluorescence was read on a GeneArray Scanner (Affymetrix), an argon laser detector. The GAPDH and actin 3':5' ratios of the amplified aRNA probes were normally between 2.5 and 10.

### Microarray data analysis

The microarray data in this report are available at [www.ncbi.nlm.nih.gov/geo](http://www.ncbi.nlm.nih.gov/geo), accession number GSE8563. The raw probe-level chip data (CEL files) were normalized by the robust multiarray average algorithm (30) using the ExpressionFileCreator module of the GenePattern 2.0 software package (31). Further analysis was performed using the MultiPlot module in GenePattern (R. Melamed and G. Hyatt, unpublished data). Random data sets were generated on a Gaussian distribution created for each gene. This distribution was centered on the gene-wise mean across all samples, with a SD that was the mean of the per-class (class = set of replicates) SDs for that gene. The false discovery rate is the frequency at which a given fold change (FC) value is higher in random data than in experimental data, for FC increments of 0.1. Values of *p* were calculated using Welch's *t* test.

## Results

### Reduced MEC numbers and aberrant organization in *LTβR*-deficient thymi

To address the question of whether the LT pathway affects the cellular composition of the thymus, we used flow cytometry to perform a thorough accounting of the numbers of stromal cells in individual wild-type (WT), *LTβR*<sup>-/-</sup> and *LTα*<sup>-/-</sup> thymi. As shown in Fig. 1A, we could identify and count cortical epithelial cells (CECs), MHC class II-high and -low MECs, *Aire*-expressing MHC class II-high MECs, dendritic cells (DCs), macrophages, fibroblasts and endothelial cells. The numbers of MECs, of all subsets, were significantly lower in *LTβR*<sup>-/-</sup> than in WT thymi (Table I). This difference was most significant when comparing the numbers of *Aire*-expressing class II-high MECs (Fig. 1B). However, MEC numbers were not similarly affected in *LTα*<sup>-/-</sup> thymi, which contained near WT levels of all subsets. Most other cell populations we evaluated were of comparable abundance in all mice examined (Table I), demonstrating an effect of *LTβR* specifically on MECs.

To determine whether thymus architecture was affected by deficiencies in the LT pathway, we stained sections from WT, *LTβR*<sup>-/-</sup> and *LTα*<sup>-/-</sup> thymi with reagents recognizing MEC markers and analyzed them by confocal microscopy. The distribution of keratin (K) 5 and K8 allowed distinction of K8<sup>+</sup> CEC and K5<sup>+</sup> MEC as previously reported (32). However, in contrast to

in each of three individual thymi. \*, *p* < 0.00026 by Student's *t* test. C, Cryosections of WT, *LTβR*<sup>-/-</sup>, or *LTα*<sup>-/-</sup> thymi were stained with UEA-1 (medullary subset, green), anti-K5 (medulla, red), and anti-K8 (cortex, blue) and images were acquired at low magnification. D, Anti-*Aire* (green) staining of WT, *LTβR*<sup>-/-</sup>, and *LTα*<sup>-/-</sup> thymi at low magnification. Cortical and medullary regions were delineated by K5 staining (data not shown). E, Anti-*Aire* (green), anti-K5 (red), and anti-K8 (blue) staining of WT, *LTβR*<sup>-/-</sup>, and *LTα*<sup>-/-</sup> thymi at high magnification. Images are representative of two independent experiments. \*, MEC-free areas containing lymphocytes. C, Cortex; M, medulla. WT immunofluorescence controls in C-E were littermates of *LTβR*<sup>-/-</sup> animals.

Table I. Cell numbers of thymic subsets in WT- and LT-deficient animals<sup>a</sup>

	<i>LTβR</i> <sup>+/+</sup>	<i>LTβR</i> <sup>-/-</sup>	<i>p</i>	<i>LTα</i> <sup>+/+</sup>	<i>LTα</i> <sup>-/-</sup>	<i>p</i>
Total thymus cells (×10 <sup>-8</sup> )	3.13 ± 0.522	2.95 ± 0.185	0.6028	2.39 ± 0.610	2.10 ± 0.676	0.6083
CD45 <sup>-</sup> cells (×10 <sup>-6</sup> )	3.07 ± 0.808	1.97 ± 0.424	0.1050	1.75 ± 0.375	1.67 ± 0.639	0.8520
CECs (×10 <sup>-5</sup> )	3.10 ± 0.847	2.51 ± 0.445	0.3444	2.86 ± 0.784	2.91 ± 2.05	0.9732
Total MECs (×10 <sup>-5</sup> )	4.49 ± 0.482	2.13 ± 0.419	<b>0.0031<sup>b</sup></b>	2.82 ± 0.47	2.74 ± 0.647	0.8710
Class II <sup>low</sup> MECs (×10 <sup>-5</sup> )	1.90 ± 0.26	1.10 ± 0.297	<b>0.0251</b>	1.27 ± 0.222	1.11 ± 0.294	0.4954
Class II <sup>high</sup> MECs (×10 <sup>-5</sup> )	2.50 ± 0.223	0.992 ± 0.107	<b>0.0005</b>	1.29 ± 0.202	1.29 ± 0.241	0.9910
Aire <sup>-</sup> class II <sup>high</sup> MECs (×10 <sup>-5</sup> )	1.37 ± 0.146	0.571 ± 0.086	<b>0.0012</b>	0.412 ± 0.0409	0.418 ± 0.0012	0.8023
Aire <sup>+</sup> class II <sup>high</sup> MECs (×10 <sup>-4</sup> )	5.78 ± 0.435	2.27 ± 0.241	<b>0.0003</b>	8.74 ± 1.6	8.64 ± 2.4	0.9548
DCs (×10 <sup>-6</sup> )	4.47 ± 0.821	3.98 ± 0.448	0.4151	1.89 ± 0.264	1.75 ± 0.512	0.6959
Macrophages (×10 <sup>-5</sup> )	2.82 ± 0.245	2.28 ± 0.429	0.1314	5.11 ± 0.963	8.00 ± 3.81	0.2720
Endothelial cells (×10 <sup>-5</sup> )	2.58 ± 0.277	2.03 ± 0.131	<b>0.0365</b>	2.93 ± 0.558	3.11 ± 1.43	0.8484
Fibroblasts (×10 <sup>-5</sup> )	2.25 ± 1.56	2.20 ± 1.09	0.9640	0.612 ± 0.169	0.477 ± 0.159	0.3708

<sup>a</sup> Total cell numbers per thymus, average ± SD of three thymi per genotype. Values of *p* were calculated using Student's *t* test. *LTα*<sup>+/+</sup> and *LTβR*<sup>+/+</sup> cell numbers were not identical because cell numbers differed from one preparation to the next due to normal variation in the extent of thymus digestion.

<sup>b</sup> Values of *p* < 0.05 are in boldface type.

Klug et al. (32), but consistent with a recent study by Gillard et al. (33), we observed coexpression of K8 and K5 by thymic epithelial cells in the medulla of WT mice, in addition to those at the corticomedullary junction (Fig. 1, *C* and *E*). The medullary regions of *LTβR*<sup>-/-</sup> thymi were smaller and more sparsely populated by K5<sup>+</sup> MECs than were those of WT thymi (Fig. 1*C*, cf *center* and *left panels*). *Ulex europaeus* agglutinin 1 (UEA-1)-positive MECs were detected on *LTβR*<sup>-/-</sup> thymus sections at a lower frequency than on WT sections and were localized in small clusters (Fig. 1*C*), consistent with previous observations (8). Frequent MEC-free regions (e.g., those asterisked in the *center panel*, Fig. 1*E*) containing lymphocytes revealed by 4',6-diamidino-2-phenylindole staining (data not shown) were observed on *LTβR*<sup>-/-</sup> sections. *LTα*<sup>-/-</sup> thymi (Fig. 1*C*, *right panel*) tended to have small medullary islets, but were not disrupted to the extent of their *LTβR*<sup>-/-</sup> counterparts. Specific anti-Aire staining showed a clustering pattern of Aire<sup>+</sup> MECs in *LTβR*<sup>-/-</sup> thymi reminiscent of that of UEA-1<sup>+</sup> MECs, in contrast to the even distribution throughout medullary areas in WT or *LTα*<sup>-/-</sup> mice (Fig. 1*D*). The characteristic punctate, nuclear localization of Aire was apparent in MECs of *LTβR*<sup>-/-</sup> and *LTα*<sup>-/-</sup> mice at fluorescent intensities similar to those of WT littermates (Fig. 1*E*), indicating normal cellular localization and expression levels.

#### Normal Aire protein levels in MECs of mice lacking LT pathway members

The amount of Aire in MECs of WT, *LTβR*<sup>-/-</sup> and *LTα*<sup>-/-</sup> thymi was compared by intracellular staining. Although MEC numbers were reduced in *LTβR*<sup>-/-</sup> thymi, the amount of Aire expressed by the remaining MECs was at the WT level, as it was in *LTα*<sup>-/-</sup> MECs (Fig. 2*A*). Calculating the mean fluorescence intensities (MFIs) of the Aire-positive, class II-high MECs confirmed this observation (Fig. 2*B*).

#### LT pathway effects on MEC gene expression profiles

To further examine the effect of a deficiency in LT pathway members on MECs, we performed gene expression-profiling using Affymetrix Mouse Genome 430 2.0 microarrays, which represent ~34,000 genes, essentially the entire mouse genome. Using flow cytometry, we isolated MECs of the phenotype CD45<sup>-</sup>G8.8<sup>+</sup>Ly51<sup>int</sup>Ab<sup>high</sup> from single-cell suspensions of thymi from individual *LTβR*<sup>-/-</sup> and *LTα*<sup>-/-</sup> animals, as well as from WT littermate controls. RNA prepared from these MEC isolates was amplified and biotinylated, then used to probe the Affymetrix chips. MECs from *aire*<sup>-/-</sup> and WT littermate controls were subjected to microarray analysis in the same manner, to permit direct

comparison of the effects of Aire vs LT-pathway deficiencies. Three WT/KO pairs for each genotype were analyzed, all mice being males of 3–4.5 wk of age on the B6 genetic background.

Fig. 3*A* displays expression values for all genes on the 430 2.0 microarrays, plotting average levels of expression of a given gene in MECs from KO vs WT littermates. *Aire* expression was not substantially affected in the LT KOs, as indicated by its proximity to the *x = y* diagonal in the top two plots of Fig. 3*A*, confirming the flow cytometric data of Fig. 2. Many more genes had a different expression level in WT vs Aire-KO MECs than in WT vs *LTβR*- or *LTα*-KO MECs. Although the numbers of genes that were changed by at least 2-fold in the *LTβR* or *LTα* comparisons were quite low in relation to those in the Aire comparison (Fig. 3*A*), they were still not as low as were found with random data (data not shown; at most, five genes with a FC > 2 and four genes with a FC < 0.5).

We wondered whether the LT-controlled genes were a subset of those affected by Aire or, rather, represented a distinct group. The FC vs FC plots in Fig. 3*B* demonstrate that different sets of genes were affected by the LT pathway and by Aire, as revealed by the lack of genes on the *x = y* diagonal in the upper two plots. However, comparison of the effects of *LTβR* and *LTα* generated a very different profile, with many genes along the *x = y* diagonal (Fig. 3*B*, *lower panel*). In fact, a linear regression on these data produced a line with a slope of 1.002, pointing to an overall trend of *LTβR* and *LTα* regulating very similar genes. To further compare Aire's effects on gene expression with those of LT pathway members, we calculated the mean *LTβR* WT/KO and *LTα* WT/KO FC values for the 1,383 genes having an Aire WT/KO FC of more than two and obtained values of 1.012 for *LTβR* and 1.020 for *LTα*. For the 408 genes with an Aire WT/KO FC < 0.5, the mean FC values were 1.038 for *LTβR* and 1.001 for *LTα*. Therefore, the group of genes most affected by Aire was, overall, minimally affected by either *LTβR* or *LTα*.

The FC vs FC plots comparing the effects of *LTβR* and *LTα* (Fig. 3*B*) revealed several genes whose expression was uniquely regulated by either *LTα* or *LTβR*, but not by both. There were 27 probe sets with a *LTα* WT/KO FC of >2 or <0.5, but a *LTβR* WT/KO FC of between 1.25 and 0.8. These 27 probe sets were specific for 24 unique genes and we considered the expression of these loci to be dependent on *LTα* but not on *LTβR*. Of these genes, 13 mapped to chromosome 17, in or near the MHC. This phenomenon may have been an artifact generated by using the *LTα* KO, considering that the *LTα* gene itself is located in the MHC. Because this KO was produced by gene targeting in embryonic stem cells of the 129 strain (4), followed by backcrossing

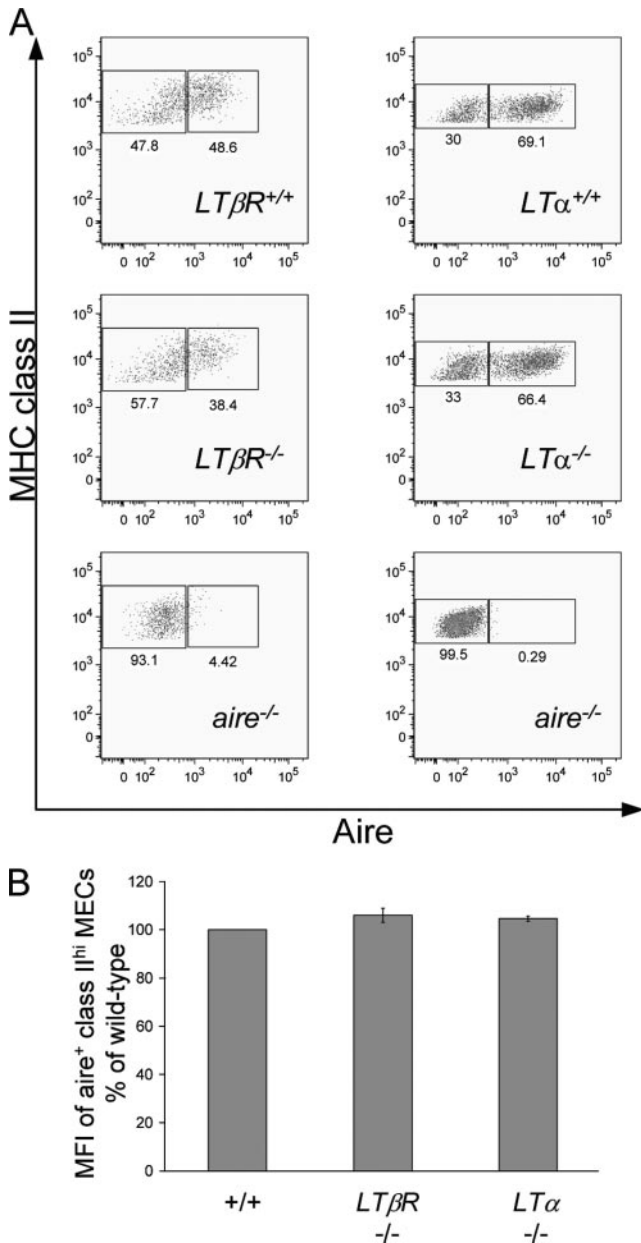


**FIGURE 2.** Aire protein levels are unaffected in MECs of mice with LT pathway deficiencies. *A*, Assessment of Aire protein levels by intracellular staining with rat anti-Aire mAb. Cells plotted are CD45<sup>-</sup>G8.8<sup>+</sup>Ly51<sup>int</sup>MHC class II<sup>high</sup>. *Aire*<sup>-/-</sup> thymi were stained as negative controls. Plots are representative of three animals of each genotype. KO and corresponding WT controls were littermates. *B*, MFIs of the CD45<sup>-</sup>G8.8<sup>+</sup>Ly51<sup>int</sup>MHC class II<sup>high</sup>Aire<sup>+</sup> cell populations were determined for each individual, and *LTβR*<sup>-/-</sup> and *LTα*<sup>-/-</sup> MFIs were compared with WT littermate controls. Bars represent the average ± SD of the relative MFIs for each of three individual thymi. Brightness and proportion of Aire<sup>+</sup> MECs differ slightly from experiment to experiment due to normal variation in the extent of thymic digestion and intracellular Aire staining.

to mice of the B6 strain, some genes from the 129 MHC region were probably carried along with the KO allele. Although both the B6 and 129 strains bear an H-2<sup>b</sup> MHC haplotype, these regions are not identical. Any genes in the region whose transcription is regulated differentially between the two strains would appear to be expressed differentially between *LTα* KO and WT mice. In addition, the neomycin-resistance cassette present in this *LTα* KO affects gene transcription (34), further suggesting that some of the

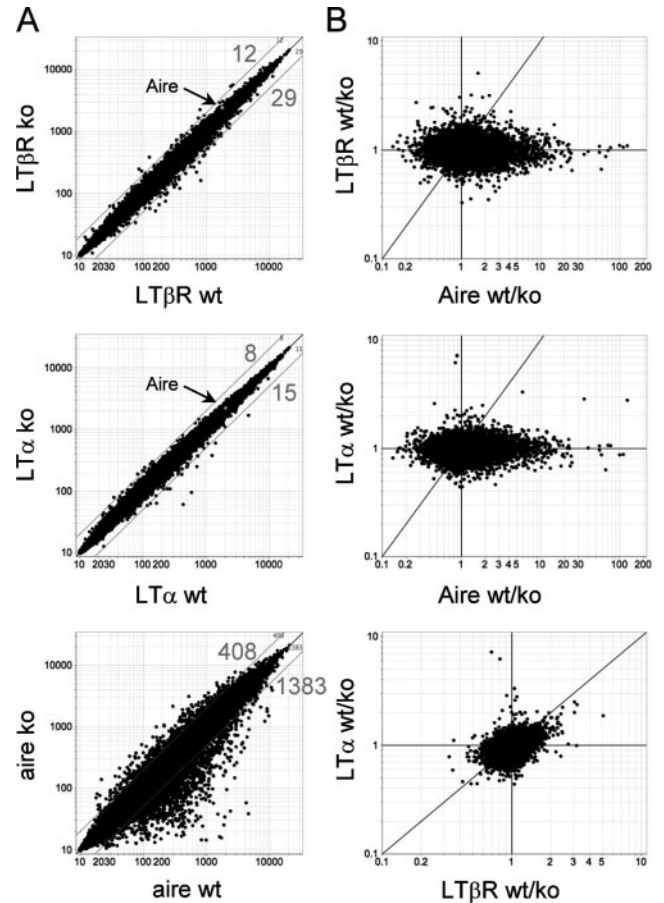


**FIGURE 3.** Gene expression profiling of MECs from mice deficient in LT pathway components vs Aire. *A*, Two-dimensional scatter plots of gene expression values for all genes on the mouse 430 2.0 microarray, comparing expression in KO and WT littermate controls. Each expression value is the mean of three independent replicate values. Gray diamonds indicate the location of Aire on the top two plots. Gray lines mark arbitrary FC cutoffs of 2 and 0.5, with gray numbers showing how many genes have FC values surpassing the cutoffs. *B*, KO vs WT expression value ratio comparisons (derived from the average expression values in *A*) for all genes on the mouse 430 2.0 microarray. The diagonal line on each plot denotes  $x = y$ . Note the different x-axis scale on the bottom plot.

gene expression differences observed for the *LTα* KO may be experimental artifacts. Among the 12 genes with a *LTβR* WT/KO FC of >2 or <0.5 but a *LTα* WT/KO FC of between 1.25 and 0.8, 4 were found on chromosome 6, near the *LTβR* gene.

In total, there were only 80 genes whose *LTα* WT/KO FC or *LTβR* WT/KO FC was >2 or <0.5. Clearly, then, LT signals do not promote large-scale up-regulation of PTA expression, as does Aire (17, 22). For example, the expression level of the PTA insulin 2 did not differ by >1.2-fold in either LT WT/KO comparison nor did insulin 1 expression. These findings do not support the recent suggestion of the Fu group (19) that *LTβR* is involved in an Aire-independent PTA expression pathway in MECs. Their conclusion was based on the observation that expression of one Ag, type II collagen (CII), was regulated by the LT pathway, but not by Aire. The microarray data presented here indicated that the level of *CII* transcription was essentially unaffected in the LT KO. The mean relative expression level of CII in the *LTα* KO MECs was 81.24 vs 90.08 in the WT littermates. The expression in *LTβR* KO MECs was 97.98 vs 92.22 in the WT littermates. The Fu group's finding (19) may have resulted from taking *K14* gene expression as a control for the RT-PCR analyses. In fact, our microarray data

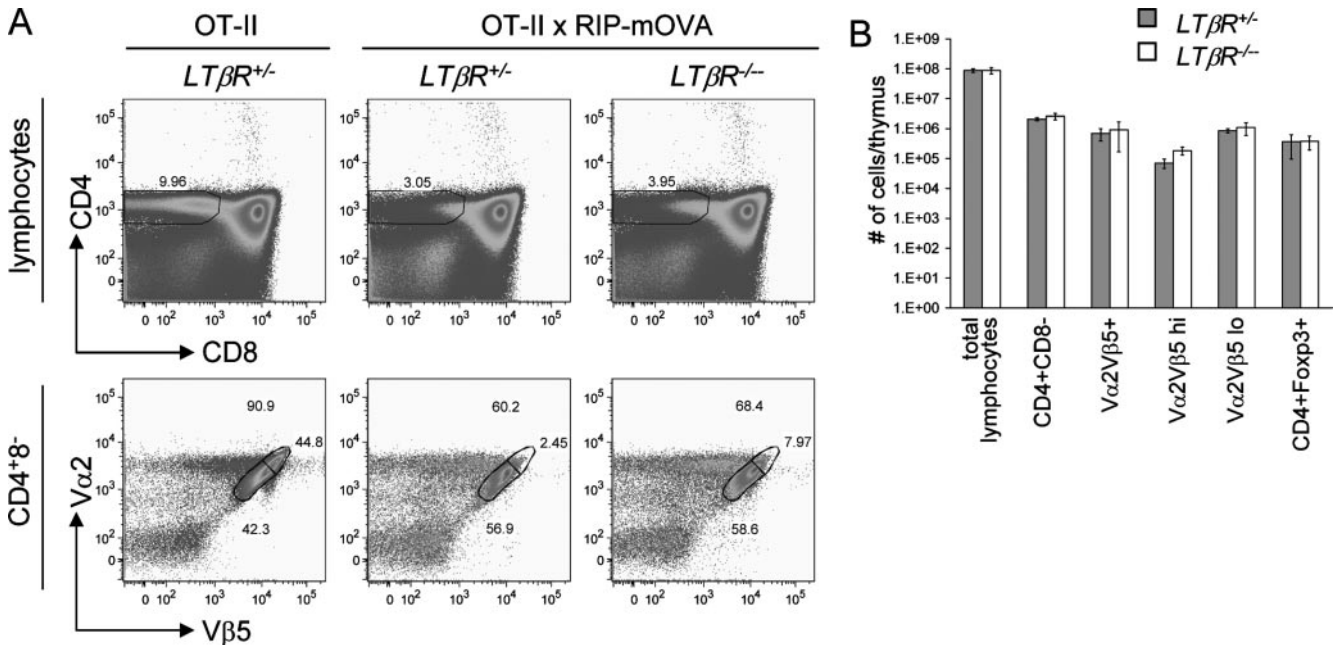


**FIGURE 4.** Clonal deletion of self-reactive thymocytes was only slightly altered in *LTβR*-deficient animals. *A*, Flow cytometric plots showing CD4 and CD8 expression by total thymic lymphocytes (*top row*) and Vα2/Vβ5 OT-II clonotype expression by CD4 single-positive thymocytes (*bottom row*). Representative of three independent experiments. *B*, Total number of cells of each indicated subset per thymus in mice of each genotype. Each bar represents the average ± SD of the cell numbers in each of three individual thymi. All mice were between 4 and 6 wk of age and were age and gender matched.

revealed an increase (~1.3-fold) in *K14* expression in the *LTβR* KO, which could well explain an augmentation in *CII* relative to *K14* expression.

Lists of genes whose expression was affected by *LTβR* or *LTα* can be found in the supplemental material.<sup>4</sup> Among the loci regulated by *LTα*, *LTβR*, or both, were those encoding proteins involved in the control of cell structure, such as epiplakin 1 and cortactin-binding protein 2. Other genes encoded proteins mediating cell-cell contact, including cadherin 2 and protocadherins 17 and 20. That the LT pathway regulates these types of genes is consistent with our immunofluorescence data and with the conclusion of Boehm et al. (8) that it is involved in controlling MEC organization within the medulla.

#### The LT pathway has little influence on thymocyte clonal deletion

Although LT did not affect *aire* or PTA gene expression, we wondered whether it might somehow control another important function of MECs, clonal deletion of self-reactive thymocytes. To evaluate the effect of LT deficiency on clonal deletion, we bred *LTβR*-deficient mice to mice transgenic for the rat insulin promoter (RIP)-mOVA Ag and the OT-II TCR. OT-II recognizes the 323–339 peptide from chicken OVA in the context of the MHC class II molecule A<sup>b</sup> (35). Thus, most single-positive thymocytes (Fig. 4*A*, *left panels*) and mature T cells (data not shown) in OT-II-transgenic mice are CD4<sup>+</sup> and express a high level of the OT-II clonotype Vα2/Vβ5. The RIP drives a high level of membrane-bound OVA expression in the pancreas and lower-level expression in the thymus and kidney (36). In double-transgenic mice, most OT-II thymocytes, in particular those displaying high levels of clonotype, were clonally deleted (Fig. 4*A*, *center panels*) since they encounter their cognate Ag OVA during differentiation in the thymus. Clonal deletion in *LTβR*-deficient mice was also very effective (Fig. 4*A*, *right panels*). There was a slight, but consistent, increase in the fraction of OVA-specific OT-II thymocytes, but this was minimally reflected

in the absolute numbers of CD4 single-positive and Vα2/Vβ5 clonotype-high and -low thymocytes (Fig. 4*B*). The number of Foxp3<sup>+</sup>CD4<sup>+</sup> regulatory T cells was also unaffected by the absence of *LTβR* (Fig. 4*B*).

Previously, Aire was found to be necessary for normal clonal deletion in OT-II/RIP-mOVA double-transgenic animals as well as in several other TCR neo-self-Ag double-transgenic systems (37, 38), in some cases independently of Aire's regulation of PTA expression (37, 39, 40). If *LTβR* does influence clonal deletion, it does so only very weakly, demonstrating that, in addition to having no influence on Aire's regulation of PTA expression, the LT pathway also does not significantly influence its regulation of clonal deletion.

## Discussion

We have analyzed the effects of deficiencies in LT pathway components on MEC number, organization, and function to resolve conflicting prior conclusions on these issues.

Our examinations of MEC numbers by flow cytometry and MEC distribution by immunofluorescence revealed a significant decrease in MEC numbers in *LTβR* KO and abnormal medullary architecture in both *LTβR* and *LTα* KO. These observations were consistent with those of Boehm et al. (8), who compared, by both immunohistochemistry and flow cytometry, the number and distribution of MECs in thymi of *LTβR* KO mice and WT littermates, demonstrating that there were significantly fewer MECs, exhibiting a disrupted localization pattern, in the former. Our finding that MEC numbers were reduced in *LTβR* KO, but not in *LTα* KO, thymi points to a role for another ligand, or ligands, of *LTβR* in controlling the MEC number. This is also the case for the findings of Boehm et al. (8). In addition to examining *LTβR* KO animals, they also studied *LTβ* KO and *LTβ*/LIGHT double-KO mice, finding that UEA-1-positive MECs from those KO mice were present at normal numbers, but displayed the same abnormal organization as those in the *LTβR* KO. Based on their observations, it seems that LIGHT, the only other known *LTβR* ligand, may not have much

<sup>4</sup> The online version of this article contains supplemental material.

of an effect on MEC distribution and that another, as-yet-unidentified ligand may be involved. Analysis of LIGHT single-knockout thymi would strengthen this conclusion. A search for other thymic ligands for LT $\beta$ R, perhaps using LT $\beta$ R-FC fusion proteins (41), may also prove fruitful.

In agreement with our findings, Rossi et al. (42) recently found, using immunofluorescence, normal numbers of Aire-expressing MECs in thymi of LT $\alpha$ <sup>-/-</sup> animals. The Fu group (9) came to a somewhat different conclusion on this point. They did find normal numbers of MECs in the LT $\alpha$ <sup>-/-</sup> thymi, as Rossi et al. (42) and we did; however, relying on visual comparisons of immunofluorescent labeling of WT and LT $\alpha$ -KO thymus sections, they concluded that the distribution of UEA-1<sup>+</sup> MECs in the latter was normal, which differed from our results. They did not show immunofluorescence data for LT $\beta$ R KOs, nor did they include LT $\beta$  or LIGHT KOs in their analyses. They also did not perform flow cytometry to assess MEC numbers.

Boehm et al. (8) and the Fu group (9) also examined the expression of Aire and PTAs in mice deficient in LT pathway components. Boehm et al. (8) cytofluorimetrically isolated MECs from WT and LT $\beta$ R KO thymi and performed semiquantitative RT-PCR for transcripts encoding Aire, insulin, and several other PTAs. They observed no differences in gene expression levels in MECs of WT and KO mice. The Fu group assayed transcription of *aire* and *insulin* by quantitative RT-PCR of cDNA from whole, unfractionated thymi from LT $\beta$ R- and LT $\alpha$ -deficient mice. They observed ~3- to 6-fold lower levels of Aire and insulin mRNA in both KOs. Because they performed their analyses on whole thymi, rather than on sorted MECs, it is possible, in the case of the LT $\beta$ R KOs, that they were measuring deficiencies in total MEC number rather than Aire levels expressed by MECs. Furthermore, Aire<sup>+</sup> MECs make up only ~0.01–0.03% of the total cells in WT thymi; therefore, these assays may have been close to the limit of detection for Aire and insulin, leading to imprecise results. This may explain why, in the case of the LT $\alpha$ -deficient thymi, in which MEC numbers were normal, that the Fu group (9) still observed lower Aire and PTA expression levels. In addition, from immunofluorescent staining of LT $\alpha$ -deficient thymus sections with polyclonal anti-Aire Ab, the Fu group concluded that Aire protein levels were much reduced; however, no quantification was performed nor was an Aire-deficient thymus control included.

The view of the Fu group (9, 19, 20), that the LT pathway controls Aire and PTA expression, seems to have taken hold in the literature (21–28). However, our results on Aire expression by flow cytometry, immunofluorescence and gene expression-profiling of isolated MECs were consistent with those of Boehm et al. (8). We observed Aire protein at normal levels in its expected punctate nuclear distribution (43, 44) in LT $\beta$ R<sup>-/-</sup> and LT $\alpha$ <sup>-/-</sup> thymus sections, rather than in the atypical perivascular localization shown by Chin et al. (9). Like Boehm et al. (8), we found no difference in Aire expression, at either the protein or transcript level, in LT $\beta$ R- or LT $\alpha$ -deficient MECs. Additionally, our microarray data revealed that only a few PTA transcripts were controlled by the LT pathway and that there was little overlap in the genes regulated by Aire and the LT pathway.

Control of Aire and subsequent PTA expression is, then, independent of the LT pathway. However, recent work by Rossi et al. (42) has proposed that another TNF/TNFR family pathway may be responsible for these phenomena. They found that the RANK ligand, produced by CD4<sup>+</sup>3<sup>-</sup> lymphoid tissue inducer cells, was required for induction of Aire and PTA expression by MECs that express RANK (42).

In conclusion, the LT pathway remains an important player in the domain of thymus development/organization and appears to

exit as a critical protagonist in the realm of Aire-mediated thymocyte tolerance.

## Acknowledgments

We thank Rachel Melamed for assistance with microarray data analysis, Dr. Hamish Scott for his gift of anti-*aire* Ab, and Dr. Yang-Xin Fu for his gift of LT $\beta$ R knockout mice.

## Disclosures

The authors have no financial conflict of interest.

## References

- Ware, C. F. 2005. Network communications: lymphotoxins, LIGHT, and TNF. *Annu Rev. Immunol.* 23: 787–819.
- Li, C., P. S. Norris, C. Z. Ni, M. L. Havert, E. M. Chiong, B. R. Tran, E. Cabezas, J. C. Reed, A. C. Satterthwait, C. F. Ware, and K. R. Ely. 2003. Structurally distinct recognition motifs in lymphotoxin- $\beta$  receptor and CD40 for tumor necrosis factor receptor-associated factor (TRAF)-mediated signaling. *J. Biol. Chem.* 278: 50523–50529.
- Dejardin, E., N. M. Droin, M. Delhase, E. Haas, Y. Cao, C. Makris, Z. W. Li, M. Karin, C. F. Ware, and D. R. Green. 2002. The lymphotoxin- $\beta$  receptor induces different patterns of gene expression via two NF- $\kappa$ B pathways. *Immunity* 17: 525–535.
- De Togni, P., J. Goellner, N. H. Ruddle, P. R. Streeter, A. Fick, S. Mariathasan, S. C. Smith, R. Carlson, L. P. Shornick, J. Strauss-Schoenberger, et al. 1994. Abnormal development of peripheral lymphoid organs in mice deficient in lymphotoxin. *Science* 264: 667–669.
- Koni, P. A., R. Sacca, P. Lawton, J. L. Browning, N. H. Ruddle, and R. A. Flavell. 1997. Distinct roles in lymphoid organogenesis for lymphotoxins  $\alpha$  and  $\beta$  revealed in lymphotoxin  $\beta$ -deficient mice. *Immunity* 6: 491–500.
- Futterer, A., K. Mink, A. Luz, M. H. Kosco-Vilbois, and K. Pfeffer. 1998. The lymphotoxin  $\beta$  receptor controls organogenesis and affinity maturation in peripheral lymphoid tissues. *Immunity* 9: 59–70.
- Banks, T. A., B. T. Rouse, M. K. Kerley, P. J. Blair, V. L. Godfrey, N. A. Kuklin, D. M. Bouley, J. Thomas, S. Kanangat, and M. L. Mucenski. 1995. Lymphotoxin- $\alpha$ -deficient mice: effects on secondary lymphoid organ development and humoral immune responsiveness. *J. Immunol.* 155: 1685–1693.
- Boehm, T., S. Scheu, K. Pfeffer, and C. C. Bleul. 2003. Thymic medullary epithelial cell differentiation, thymocyte emigration, and the control of autoimmunity require lympho-epithelial cross talk via LT $\beta$ R. *J. Exp. Med.* 198: 757–769.
- Chin, R. K., J. C. Lo, O. Kim, S. E. Blink, P. A. Christiansen, P. Peterson, Y. Wang, C. Ware, and Y. X. Fu. 2003. Lymphotoxin pathway directs thymic Aire expression. *Nat. Immunol.* 4: 1121–1127.
- Shinkura, R., K. Kitada, F. Matsuda, K. Tashiro, K. Ikuta, M. Suzuki, K. Kogishi, T. Serikawa, and T. Honjo. 1999. A lymphoplasia is caused by a point mutation in the mouse gene encoding NF- $\kappa$ B-inducing kinase. *Nat. Genet.* 22: 74–77.
- Yin, L., L. Wu, H. Wesche, C. D. Arthur, J. M. White, D. V. Goeddel, and R. D. Schreiber. 2001. Defective lymphotoxin- $\beta$  receptor-induced NF- $\kappa$ B transcriptional activity in NIK-deficient mice. *Science* 291: 2162–2165.
- Burkly, L., C. Hession, L. Ogata, C. Reilly, L. A. Marconi, D. Olson, R. Tizard, R. Cate, and D. Lo. 1995. Expression of reIB is required for the development of thymic medulla and dendritic cells. *Nature* 373: 531–536.
- Browning, J. L., I. D. Sizing, P. Lawton, P. R. Bourdon, P. D. Rennert, G. R. Majeau, C. M. Ambrose, C. Hession, K. Miatkowski, D. A. Griffiths, et al. 1997. Characterization of lymphotoxin- $\alpha$  $\beta$  complexes on the surface of mouse lymphocytes. *J. Immunol.* 159: 3288–3298.
- Mauri, D. N., R. Ebner, R. I. Montgomery, K. D. Kochel, T. C. Cheung, G. L. Yu, S. Ruben, M. Murphy, R. J. Eisenberg, G. H. Cohen, et al. 1998. LIGHT, a new member of the TNF superfamily, and lymphotoxin  $\alpha$  are ligands for herpesvirus entry mediator. *Immunity* 8: 21–30.
- Browning, J. L., and L. E. French. 2002. Visualization of lymphotoxin- $\beta$  and lymphotoxin- $\beta$  receptor expression in mouse embryos. *J. Immunol.* 168: 5079–5087.
- Derbinski, J., A. Schulte, B. Kyewski, and L. Klein. 2001. Promiscuous gene expression in medullary thymic epithelial cells mirrors the peripheral self. *Nat. Immunol.* 2: 1032–1039.
- Anderson, M. S., E. S. Venanzi, L. Klein, Z. Chen, S. P. Berzins, S. J. Turley, H. von Boehmer, R. Bronson, A. Dierich, C. Benoist, and D. Mathis. 2002. Projection of an immunological self shadow within the thymus by the aire protein. *Science* 298: 1395–1401.
- Ramsey, C., O. Winqvist, L. Puhakka, M. Halonen, A. Moro, O. Kampe, P. Eskelin, M. Pelto-Huikko, and L. Peltonen. 2002. Aire deficient mice develop multiple features of APECED phenotype and show altered immune response. *Hum. Mol. Genet.* 11: 397–409.
- Chin, R. K., M. Zhu, P. A. Christiansen, W. Liu, C. Ware, L. Peltonen, X. Zhang, L. Guo, S. Han, B. Zheng, and Y. X. Fu. 2006. Lymphotoxin pathway-directed, autoimmune regulator-independent central tolerance to arthritogenic collagen. *J. Immunol.* 177: 290–297.
- Zhu, M., R. K. Chin, P. A. Christiansen, J. C. Lo, X. Liu, C. Ware, U. Siebenlist, and Y. X. Fu. 2006. NF- $\kappa$ B2 is required for the establishment of central tolerance through an Aire-dependent pathway. *J. Clin. Invest.* 116: 2964–2971.
- Sillanpaa, N., C. G. Magureanu, A. Murumagi, A. Reinikainen, A. West, A. Manninen, M. Lahti, A. Ranki, K. Saksela, K. Krohn, et al. 2004. Autoimmune

- regulator induced changes in the gene expression profile of human monocyte-dendritic cell-lineage. *Mol. Immunol.* 41: 1185–1198.
22. Derbinski, J., J. Gabler, B. Brors, S. Tierling, S. Jonnakuty, M. Hergenahn, L. Peltonen, J. Walter, and B. Kyewski. 2005. Promiscuous gene expression in thymic epithelial cells is regulated at multiple levels. *J. Exp. Med.* 202: 33–45.
  23. Pereira, L. E., P. Bostik, and A. A. Ansari. 2005. The development of mouse APECED models provides new insight into the role of Aire in immune regulation. *Clin. Dev. Immunol.* 12: 211–216.
  24. Nagafuchi, S., H. Katsuta, Y. Ohno, Y. Inoue, K. Shimoda, K. Kogawa, Y. Ikeda, R. Koyanagi-Katsuta, S. Yamasaki, H. Tominaga, et al. 2005. Mitogen-activated protein kinase pathway controls autoimmune regulator (AIRE) gene expression in granulocyte colony stimulating factor (GM-CSF)-stimulated myelomonocytic leukemia OTC-4 cells. *Immunol. Lett.* 99: 130–135.
  25. Nagafuchi, S., H. Katsuta, R. Koyanagi-Katsuta, S. Yamasaki, Y. Inoue, K. Shimoda, Y. Ikeda, M. Shindo, E. Yoshida, T. Matsuo, et al. 2006. Autoimmune regulator (AIRE) gene is expressed in human activated CD4<sup>+</sup> T-cells and regulated by mitogen-activated protein kinase pathway. *Microbiol. Immunol.* 50: 979–987.
  26. Clark, R. A., K. Yamanaka, M. Bai, R. Dowgiert, and T. S. Kupper. 2005. Human skin cells support thymus-independent T cell development. *J. Clin. Invest.* 115: 3239–3249.
  27. Cavadini, P., W. Vermi, F. Facchetti, S. Fontana, S. Nagafuchi, E. Mazzolari, A. Sediva, V. Marrella, A. Villa, A. Fischer, L. D. Notarangelo, and R. Badolato. 2005. Aire deficiency in thymus of 2 patients with Omenn syndrome. *J. Clin. Invest.* 115: 728–732.
  28. Notarangelo, L. D., E. Gambineri, and R. Badolato. 2006. Immunodeficiencies with autoimmune consequences. *Adv. Immunol.* 89: 321–370.
  29. Gray, D. H., A. P. Chidgey, and R. L. Boyd. 2002. Analysis of thymic stromal cell populations using flow cytometry. *J. Immunol. Methods* 260: 15–28.
  30. Irizarry, R. A., B. Hobbs, F. Collin, Y. D. Beazer-Barclay, K. J. Antonellis, U. Scherf, and T. P. Speed. 2003. Exploration, normalization, and summaries of high density oligonucleotide array probe level data. *Biostatistics* 4: 249–264.
  31. Reich, M., T. Liefeld, J. Gould, J. Lerner, P. Tamayo, and J. P. Mesirov. 2006. GenePattern 2.0. *Nat. Genet.* 38: 500–501.
  32. Klug, D. B., C. Carter, E. Crouch, D. Roop, C. J. Conti, and E. R. Richie. 1998. Interdependence of cortical thymic epithelial cell differentiation and T-lineage commitment. *Proc. Natl. Acad. Sci. USA* 95: 11822–11827.
  33. Gillard, G. O., J. Dooley, M. Erickson, L. Peltonen, and A. G. Farr. 2007. Aire-dependent alterations in medullary thymic epithelium indicate a role for Aire in thymic epithelial differentiation. *J. Immunol.* 178: 3007–3015.
  34. Pham, C. T., D. M. MacIvor, B. A. Hug, J. W. Heusel, and T. J. Ley. 1996. Long-range disruption of gene expression by a selectable marker cassette. *Proc. Natl. Acad. Sci. USA* 93: 13090–13095.
  35. Barnden, M. J., J. Allison, W. R. Heath, and F. R. Carbone. 1998. Defective TCR expression in transgenic mice constructed using cDNA-based  $\alpha$ - and  $\beta$ -chain genes under the control of heterologous regulatory elements. *Immunol. Cell Biol.* 76: 34–40.
  36. Kurts, C., W. R. Heath, F. R. Carbone, J. Allison, J. F. Miller, and H. Kosaka. 1996. Constitutive class I-restricted exogenous presentation of self antigens in vivo. *J. Exp. Med.* 184: 923–930.
  37. Anderson, M. S., E. S. Venanzi, Z. Chen, S. P. Berzins, C. Benoist, and D. Mathis. 2005. The cellular mechanism of Aire control of T cell tolerance. *Immunity* 23: 227–239.
  38. Liston, A., S. Lesage, J. Wilson, L. Peltonen, and C. C. Goodnow. 2003. Aire regulates negative selection of organ-specific T cells. *Nat. Immunol.* 4: 350–354.
  39. Kuroda, N., T. Mitani, N. Takeda, N. Ishimaru, R. Arakaki, Y. Hayashi, Y. Bando, K. Izumi, T. Takahashi, T. Nomura, et al. 2005. Development of autoimmunity against transcriptionally unrepressed target antigen in the thymus of Aire-deficient mice. *J. Immunol.* 174: 1862–1870.
  40. Niki, S., K. Oshikawa, Y. Mouri, F. Hirota, A. Matsushima, M. Yano, H. Han, Y. Bando, K. Izumi, M. Matsumoto, K. I. Nakayama, et al. 2006. Alteration of intra-pancreatic target-organ specificity by abrogation of Aire in NOD mice. *J. Clin. Invest.* 116: 1292–1301.
  41. Rennert, P. D., J. L. Browning, R. Mebius, F. Mackay, and P. S. Hochman. 1996. Surface lymphotoxin  $\alpha\beta$  complex is required for the development of peripheral lymphoid organs. *J. Exp. Med.* 184: 1999–2006.
  42. Rossi, S. W., M. Y. Kim, A. Leibbrandt, S. M. Parnell, W. E. Jenkinson, S. H. Glanville, F. M. McConnell, H. S. Scott, J. M. Penninger, E. J. Jenkinson, et al. 2007. RANK signals from CD4<sup>+</sup>3<sup>-</sup> inducer cells regulate development of Aire-expressing epithelial cells in the thymic medulla. *J. Exp. Med.* 204: 1267–1272.
  43. Bjorsors, P., M. Peltto-Huikko, J. Kaukonen, J. Aaltonen, L. Peltonen, and I. Ulmanen. 1998. Localization of the APECED protein in distinct nuclear structures. *Hum. Mol. Genet.* 8: 259–266.
  44. Rinderle, C., H.-M. Christensen, S. Schweiger, H. Lehrach, and M.-L. Yaspo. 1998. AIRE encodes a nuclear protein co-localizing with cytoskeletal filaments: altered sub-cellular distribution of mutants lacking the PHD zinc fingers. *Hum. Mol. Genet.* 8: 277–290.